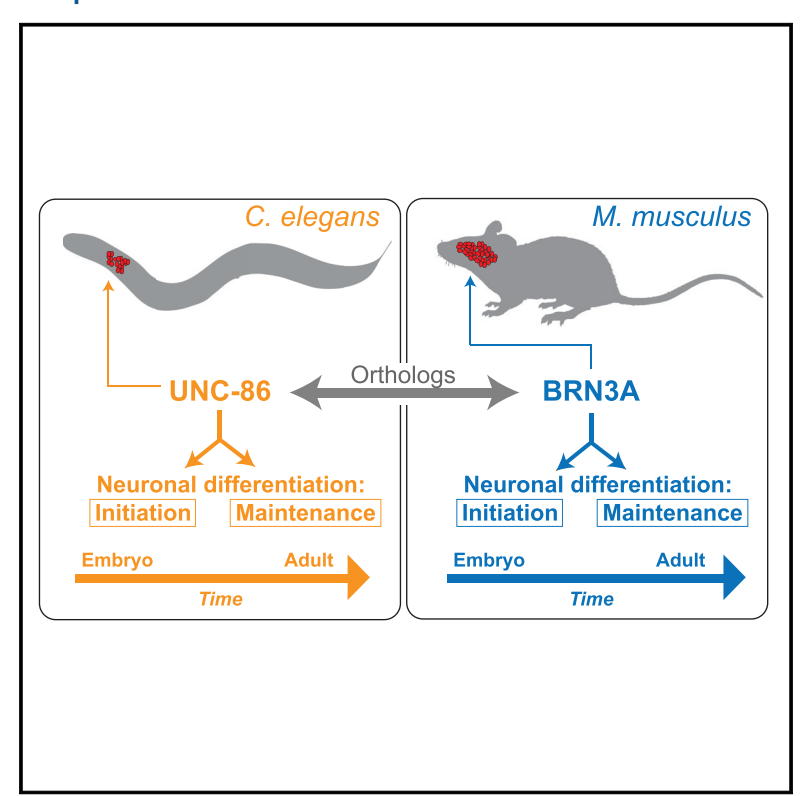
Current Biology

BRN3-type POU Homeobox Genes Maintain the Identity of Mature Postmitotic Neurons in Nematodes and Mice

Graphical Abstract



Authors

Esther Serrano-Saiz, Eduardo Leyva-Díaz, Estanislao De La Cruz, Oliver Hobert

Correspondence

esther.serrano.saiz@gmail.com (E.S.-S.), or38@columbia.edu (O.H.)

In Brief

Serrano-Saiz et al. show that two phylogenetically conserved POU homeobox genes, previously shown to be required for the initiation of specific neuronal differentiation programs, are also required to maintain neuronal identity in the adult nervous system of mice and worms.

Highlights

- Worm and mouse POU homeobox gene orthologs display similar functions
- unc-86 maintains neuronal identity in different mature neuron types in C. elegans
- Brn3a maintains the identity of Medial Habenula neurons in adult mice
- Brn3a continuously promotes survival of Medial Habenula neurons and afferents







BRN3-type POU Homeobox Genes Maintain the Identity of Mature Postmitotic Neurons in Nematodes and Mice

Esther Serrano-Saiz,1,* Eduardo Leyva-Díaz,1 Estanislao De La Cruz,1 and Oliver Hobert1,2,*

¹Department of Biological Sciences, Howard Hughes Medical Institute, Columbia University, New York, NY, USA ²Lead Contact

*Correspondence: esther.serrano.saiz@gmail.com (E.S.-S.), or38@columbia.edu (O.H.) https://doi.org/10.1016/j.cub.2018.06.045

SUMMARY

Many distinct regulatory factors have been shown to be required for the proper initiation of neuron-typespecific differentiation programs, but much less is known about the regulatory programs that maintain the differentiated state in the adult [1-3]. One possibility is that regulatory factors that initiate a terminal differentiation program during development are continuously required to maintain the differentiated state. Here, we test this hypothesis by investigating the function of two orthologous POU homeobox genes in nematodes and mice. The C. elegans POU homeobox gene unc-86 is a terminal selector that is required during development to initiate the terminal differentiation program of several distinct neuron classes [4-13]. Through post-developmental removal of unc-86 activity, we show here that unc-86 is also continuously required throughout the life of many neuron classes to maintain neuron-class-specific identity features. Similarly, the mouse unc-86 ortholog Brn3a/POU4F1 has been shown to control the initiation of the terminal differentiation program of distinct neuron types across the mouse brain, such as the medial habenular neurons [14-20]. By conditionally removing Brn3a in the adult mouse central nervous system, we show that, like its invertebrate ortholog unc-86, Brn3a is also required for the maintenance of terminal identity features of medial habenular neurons. In addition, Brn3a is required for the survival of these neurons, indicating that identity maintenance and survival are genetically linked. We conclude that the continuous expression of transcription factors is essential for the active maintenance of the differentiated state of a neuron across phylogeny.

RESULTS AND DISCUSSION

UNC-86 Maintains the Terminal Identity of Distinct Neuron Classes in *C. elegans*

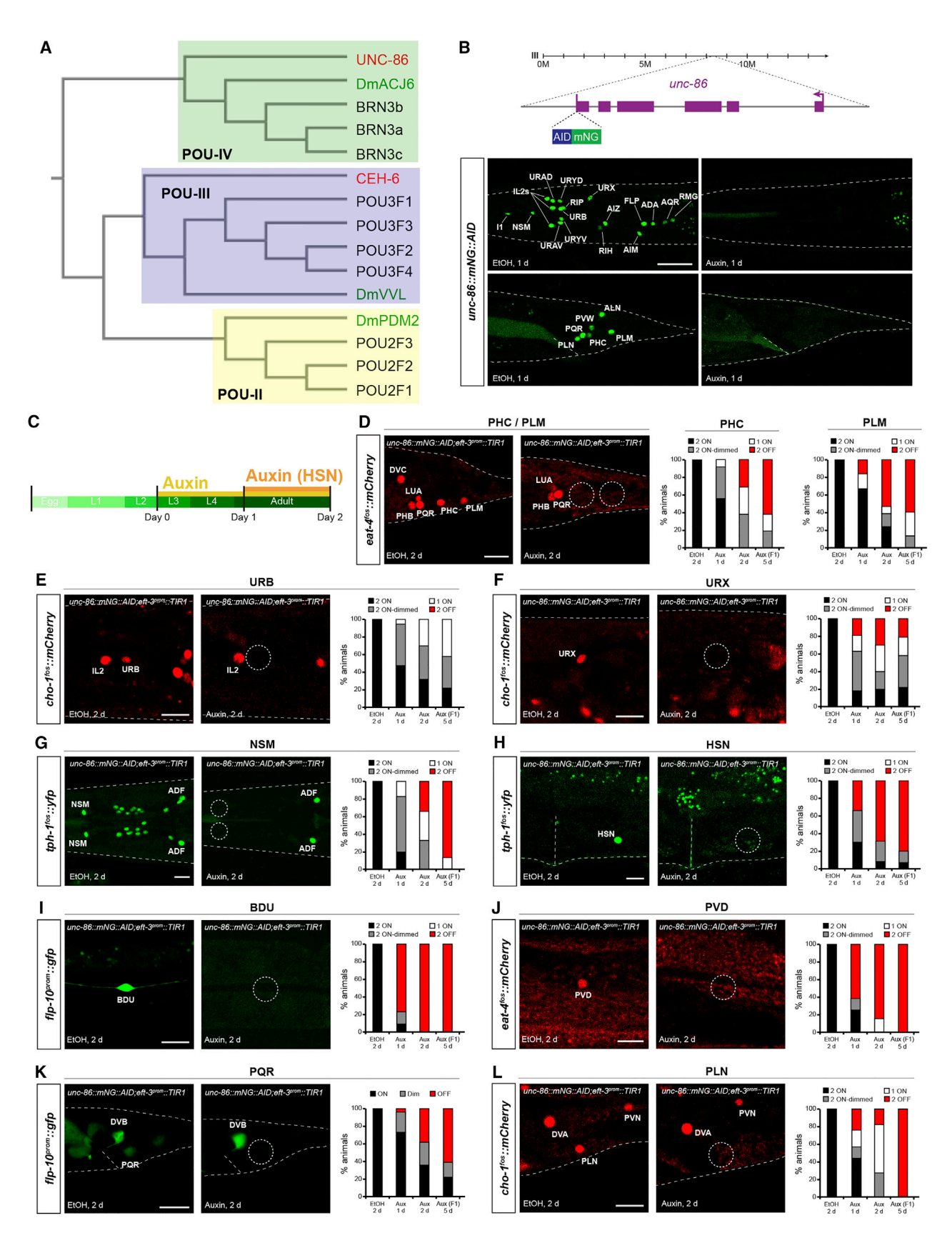
POU (Pit1/Oct1/UNC-86) homeobox genes are highly conserved transcription factors with orthologs ranging from nematodes to

mammals (Figures 1A and S1) [22]. One of the founding members of the POU homeobox gene family, the C. elegans unc-86 gene, specifies many identity aspects of more than a dozen different neuron classes during development [4-13] (summarized in Table S1). For example, unc-86 is required to specify the glutamatergic identity of 4 sensory and interneurons (as measured by the expression of the vesicular glutamate transporter eat-4/VGluT) [8] and the cholinergic identity of 7 sensory, inter-, and motor neurons (as measured by the expression of the acetylcholine synthesizing enzyme and transporters) [9, 11]. While, in most neuron classes, unc-86 expression is exclusively observed in postmitotic neurons, in some lineages, unc-86 expression initiates earlier in the lineage in neuroblasts before their terminal division (Figure S2A) [5, 23]; in several of these lineages, loss of unc-86 results in homeotic lineage duplications such that the fate of the mother cell becomes aberrantly reiterated [6] (Figure S2B). These lineage defects precluded any further investigation of unc-86 function in the postmitotic neurons generated by these lineages.

Once initiated in 31 neuron classes, unc-86 expression is maintained in 30 of these 31 neuron classes throughout larval and adult life (the exception is the SDQ neuron class, where unc-86 is transiently expressed) [5, 23]. However, the postdevelopmental role of unc-86 at later, post-developmental stages remains unknown. To address this question, we generated a conditional unc-86 allele, unc-86(ot893), that permits temporally controlled UNC-86 protein degradation using an auxin-inducible degron (AID). This system makes use of the auxin-dependent plant ubiquitin ligase TIR1, which, upon auxin supplementation, mediates proteasomal degradation of AID-tagged proteins [24]. Using CRISPR/Cas9-mediated genome engineering [25], we inserted the AID tag together with mNeonGreen at the 3' end of the unc-86 locus (Figure 1B). unc-86::mNeonGreen::AID is expressed in the same neuron classes as previously reported by antibody staining against endogenous UNC-86 protein [5](Table S1, Figure 1B); in addition, we detected expression in an extra neuron pair in the tail, the peptidergic PVW interneurons.

We crossed the *unc-86::mNeonGreen::AID* allele into a transgenic line that expresses the auxin-dependent TIR1 ubiquitously [24] which allowed us to address the following: (1) the role of *unc-86* in maintaining terminal neuronal identity features in adult worms; and (2) the postmitotic role of *unc-86* in those neuronal lineages where early *unc-86* activity prevents homeotic lineage transformations. We observed that addition of auxin to plates with worm larvae at the third larval (L3) stage resulted in the





(legend on next page)

disappearance of mNeonGreen-tagged UNC-86 protein one day after treatment (Figures 1B and 1C). Having established the efficiency of this system, we analyzed the post-development requirement of unc-86 to maintain a key neuronal identity feature, the neurotransmitter identity of multiple distinct neuron classes. To not interfere with the initial generation and specification of both the embryonic and post-embryonic unc-86(+) neuron classes, auxin was added to synchronized populations of growing worms at the L3 stage (Figure 1C)-long after all embryonically generated unc-86(+) neuron classes have differentiated and started to express their neurotransmitter identity. In the case of the analysis of the embryonically born HSN, whose serotonergic neurotransmitter identity only becomes expressed at the fourth larval stage, auxin was added to worms at the young adult stage. Expression of glutamatergic, cholinergic, serotonergic, and peptidergic markers was analyzed after 1 or 2 days on auxin (or ethanol as vehicle control) or in the F1 generation (5 days on auxin) as a control for a constitutive removal of UNC-86 (Figure 1C). We found that late larval or adult removal of UNC-86 affected the glutamatergic identity of the embryonically born PLM touch sensory neurons (as assessed by loss of expression of the vesicular glutamate transporter eat-4/VGLUT), the cholinergic identity of the embryonically born URB and URX (as assessed by loss of expression of the choline re-uptake transporter cho-1/CHT), the serotonergic identity of the embryonically born NSM and HSN (as assessed by loss of expression of the tryptophan hydroxylase tph-1/TPH1), and the peptidergic identity of the embryonically born BDU neurons (as assessed by loss of expression of a FMRFamide encoding gene, flp-10) (Figures 1D-11; Table S1). A previous analysis of constitutive unc-86 null mutants demonstrated that loss of unc-86 does not affect the expression of pan-neuronal molecular markers, indicating that loss of unc-86 does not affect neuron survival [11, 13]. Similarly, post-developmental removal of unc-86 does not affect the survival of neurons either (15/15 BDU neurons and 15/15 PVD neurons still express the pan-neuronal rab-3 marker even though they lose neurotransmitter identity).

Our conditional *unc-86* allele also allowed us to characterize the function of UNC-86 in neuron classes derived from those lineages in which aberrant earlier cell division pattern in *unc-86* null

mutants (Figure S2B) prevented the study of post-mitotic specification mechanisms. We found that after post-developmental removal of UNC-86, neurotransmitter identity was disrupted in the PVD sensory neurons (glutamatergic identity, V5 lineage), the PQR sensory neuron (peptidergic identity, Q lineage), and the T lineage sensory neurons PHCs (glutamatergic identity) and PLNs (cholinergic identity) (Figures 1D and 1J–1L). These findings demonstrate that apart from its early role in controlling neuroblast division patterns, *unc-86* is not only required during initial neuronal differentiation as previously shown, but also continuously required post-mitotically to maintain neuron type-specific identity features.

Conditional Removal of *Brn3a* Leads to the Degeneration of Adult Medial Habenular Neurons

To assess whether the role of unc-86 in both initiating and maintaining neuronal identity is phylogenetically conserved, we turned to the mouse unc-86 ortholog Brn3a/POU4F1 [14, 22, 26] (Figure 1A). Brn3a is expressed in a number of different regions of the developing and adult CNS, where it appears to have diverse functions (Table S2). We focused our analysis on Brn3a function on a phylogenetically deeply conserved structure in the diencephalon, the medial habenula [27]. Brn3a is expressed in all neurons of the medial habenula as they form in the embryo and begin to differentiate, and Brn3a has been shown to be required for this differentiation process [15]. Using antibody staining, we confirmed that Brn3a expression persists in these neurons throughout adulthood, as previously reported [15] (Figure 2C). We generated a conditional Brn3a knockout mouse (from hereon referred to as Brn3acKO) by crossing the existing previously published conditional Brn3aFloxAP allele (Figure 2A) [16] to a mouse line that expresses a tamoxifen-inducible form of Cre recombinase under the control of the ubiquitously expressed Rosa26 locus (R26^{CreER}) [29]. This approach allowed us to remove Brn3a in 8-week-old adult animals upon tamoxifen treatment. Since the *Brn3a^{FloxAP}* allele was engineered to express the human placental alkaline phosphatase (AP) gene upon Cremediated removal of Brn3a locus [16], we were able to explicitly identify the neurons in which Brn3a was removed via antibody staining against AP (Figures 2A and 2F). We treated Brn3aFloxAP

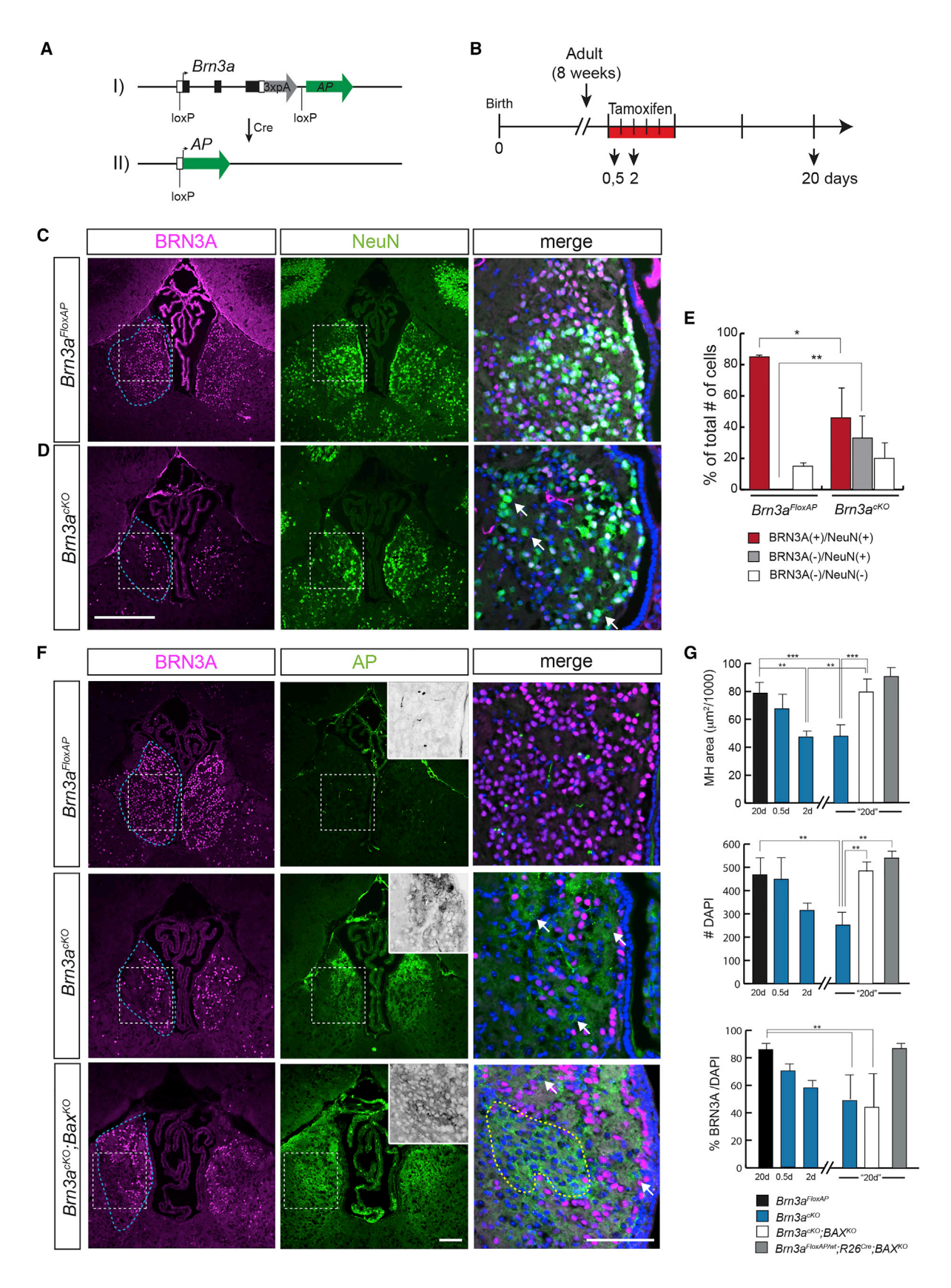
Figure 1. UNC-86 Is Required to Maintain Terminal Identity in C. elegans

(A) Phylogenetic tree of POU homeobox genes generated with T-Coffee [21]. Red: C. elegans proteins, green: Drosophila protein, black: mouse proteins. Brn3a, Brn3b, and Brn3c are also termed POU4F1, POU4F2, and POU4F3, respectively. A more detailed phylogram is shown in Figure S1.

(B) Schematic of genome-edited *unc-86* gene locus. Auxin-inducible degron (AID), mNeonGreen (mNG). Lower panels show *unc-86::mNG:::AID* expression in neurons in head (top) and tail (bottom) of the worm, which is lost after 1 day treatment with auxin (right) compared to control ethanol (vehicle) treatment (left). Lateral views of the head and tail are shown. The expression of UNC-86 is summarized in Figure S2.

(C) Schematic depicting the auxin treatment. With the exception of HSN analysis, auxin was added to synchronized populations of growing worms at the L3 stage. For analysis of tph-1 fosmid reporter expression on HSN, auxin was added to synchronized populations of growing worms at the young adult stage.

(D–L) Expression of molecular identity markers (= reporter transgenes) was analyzed in *unc-86(ot893)[unc-86::mNG::AID]*; *ieSi57[eft-3^{prom}::TIR1]* animals after 2 days on ethanol as vehicle control, 1 day or 2 days on auxin, and in the F1 generation (after 5 days on auxin). Percentage of animals that express the reporter in both cells of the respective left and right neuron pair ("2 ON" or "2 ON-dimmed") or one of the two neurons of a neuron pair ("1 ON") or in neither ("2 OFF") are indicated. On the "Aux (F1)" condition, auxin was added to synchronized populations of growing worms at the L3 stage and their F1 progeny, born and fully developed on auxin, was examined at the adult stage. Auxin was added as indicated in (C). UNC-86 is required for maintenance of *cho-1/ChT* expression (assayed with *cho-1/ChT* fosmid reporter transgene *otls544*) in the URB (E), URX (F), and PLN (L) neurons; of *tph-1/TPH1* expression (assayed with *tph-1* fosmid reporter transgene *otls517*) in the NSM (G) and HSN (H) neurons; of *flp-10* expression (assayed with *flp-10* reporter transgene *otls92*) in the BDU (I) and PQR (K) neurons; and of *eat-4/VGluT* expression (assayed with *eat-4* fosmid reporter transgene *otls518*) in the PVD (J), PHC, and PLM (D) neurons. NSM pictures show a dorso-ventral view of the worm head. Note that *tph-1* fos::yfp is expressed only in NSM and ADF neuronal pairs in the worm head, overlapping with *unc-86::mNG::AID* expression (other neurons expressing *unc-86::mNG::AID* are shown in the EtOH control image). At least 15 animals examined for each genotype. Scale bars represent 20 μm (B) and 10 μm (D–L). Table S1 shows a summary of the results and a comparison to the phenotypes observed with the *unc-86:(n486)* null allele.



(legend on next page)

(as control animals) and Brn3aFloxAP; R26CreER (= Brn3aCKO animals) with tamoxifen for 5 consecutive days and collected the brains samples 15 days later (we noted high mortality upon lengthening the time of treatment or lengthening the 15-day period after the 5-day tamoxifen treatment) (Figure 2B; see Figure S3 for non-tamoxifen treated Brn3aFloxAP). We first determined the total number of cells in the medial habenula (MH) by counting DAPI-positive nuclei in control (Brn3aFloxAP tamoxifentreated animals) and tamoxifen-treated Brn3acKO animals. We found that loss of BRN3A in adult animals results in a 50% reduction in the total number of cells compared to control Brn3aFloxAP (Figures 2C-2E and 4B). Among the surviving cells, 33% have lost BRN3A but still express NeuN (BRN3A[-]/NeuN[+]], and 46% have not lost BRN3A expression (BRN3A[+]/NeuN[+]). We conclude that loss of Brn3a function results in the degeneration of MH neurons.

To assess by which cell death pathway habenular neurons die upon removal of *Brn3a*, we crossed *Brn3a^{cKO}* animals to a mouse line carrying a targeted deletion of the *Bax* gene (from hereon referred to as *Bax^{KO}*) [30]. BAX is a pro-apoptotic protein that is implicated in the mitochondria-dependent apoptotic cell death pathway [31]. Hence, the use of the *Bax^{KO}* mice allowed us to assess whether *Brn3a* acts to prevent cell death via this specific cell death pathway and, if so, to analyze the effect of *Brn3a* removal from postmitotic neurons on neuronal identity. As done for the *Brn3a^{cKO}* animals, we treated the *Brn3a^{cKO}*; *Bax^{KO}* animals with tamoxifen for 5 days and obtained brain samples 15 days after (20 days post-tamoxifen treatment). We quantified the total number of DAPI nuclei in the MH region and found that the cell loss phenotype of *Brn3a^{cKO}* mutant was

completely rescued in the absence of *Bax* (Figures 2F, 2G, and S3C). We conclude that adult removal of *Brn3a* leads to BAX-mediated cellular apoptosis.

BRN3A Is Necessary for the Maintenance of the Terminal Identity of the Adult Medial Habenula Neurons

The prevention of cell death in Brn3acKO; BaxKO animals allowed us to assess potential roles of Brn3a in the maintenance of terminal neuronal identity independent from its role in maintaining cellular survival. A key feature of mature neurons is their neurotransmitter identity. All MH neurons are glutamatergic, expressing the vesicular glutamate transporter VGluT1 [32]. The dorsal MH (dMH) neurons are also peptidergic, expressing the Substance P neuropeptide; in contrast, the ventral MH (vMH) neurons co-transmit acetylcholine and glutamate [32, 33]. We quantified the number of VGluT1(+) cells by in situ hybridization in Brn3a^{FloxAP}, Brn3a^{cKO}, and Brn3a^{cKO};Bax^{KO} animals 20 days post-tamoxifen treatment (Figures 3B and 3D). We found a 60% reduction in the number of glutamatergic cells in $\textit{Brn3}^{\textit{cKO}}$ compared to Brn3aFloxAP, which can be explained by the cell loss in the MH of these animals (Figure 2). In the absence of cell death in Brn3a^{cKO};Bax^{KO} animals, the overall neuron number remained constant compared to Brn3aFloxAP control (Figure 2G), but we still observed a 50% reduction in the number of VGluT1(+) neurons in the MH (Figures 3B and 3D). We conclude that Brn3a is required to maintain VGluT1 expression in adult MH neurons independent of its role in preventing cell death.

Ventral MH neurons also fail to maintain their cholinergic neurotransmitter identity upon adult removal of *Bm3a*. Comparing tamoxifen-treated *Bm3a*^{FloxAP} and *Bm3a*^{cKO}:*Bax*^{KO}

Figure 2. Conditional Removal of Brn3a in Adult Brain Triggers the Degeneration of the Medial Habenula Neurons

(A) Schematic of the conditional targeting strategy. (I) Targeted locus. (II) The targeted locus after Cre-mediated excision of the *Bm3a* coding regions, which places the *AP* coding region under the control of the *Bm3a* promoter. Filled black boxes, BRN3A exons; gray box, 3 repeats of the SV40 transcription terminator; green box, human AP coding region [16].

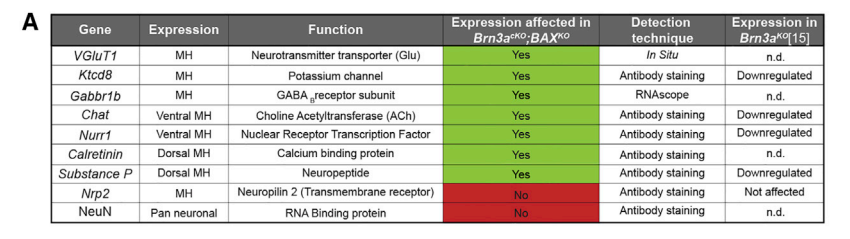
(B) Timeline for the tamoxifen treatment (see STAR Methods for further details). Control $Bm3a^{FloxAP}$ and $Bm3a^{cKO}$ adult (8 week) animals were treated with tamoxifen for 0.5, 2, and 5 days. Animals were sacrificed immediately after the treatment except for the 5-day point when we waited for 15 days after the tamoxifen treatment (20-day post-treated). Black arrows indicate the time points of euthanasia.

(C and D) BRN3A expression is reduced in $Bm3a^{CKO}$ adult mice. Co-labeling of BRN3A, NeuN and DAPI by antibody staining in tamoxifen treated $Bm3a^{FKO}$ control animals (C) and in tamoxifen treated $Bm3a^{CKO}$ adult mice (D). Adult (8 week) animals were treated with tamoxifen for 5 days and brains collected 15 days after (20 day-post treatment) (B). BRN3A and NeuN antibody co-staining reveals the presence of BRN3A(-)/NeuN(+) neurons in 20-day post-treated $Bm3a^{CKO}$ animals (white arrows). The box indicates the magnified area in the merged column. A total of 8 animals per condition were analyzed in 3 independent experiments.

(E) Quantification of BRN3A and NeuN expression after the conditional removal of Bm3a. The bars represent the percentage of neurons expressing BRN3A and NeuN relative to the total number of DAPI nuclei in the MH area in their respective genotypes (blue dashed line in C for $Bm3a^{FloxAP}$ and D for $Bm3a^{FloxAP}$). Note that there is a subpopulation of cells that do not express BRN3A or NeuN, reflecting previously reported non-neuronal cells in the MH [28]. There are no changes in the total number of these cells between the control $Bm3a^{FloxAP}$ and $Bm3a^{FloxAP}$ and Bm3

(F) The MH cell death is rescued in a Bax^{KO} background. Co-staining of BRN3A, alkaline phosphatase (AP), and DAPI control $Bm3a^{FloxAP}$, $Bm3a^{cKO}$, and $Bm3a^{cKO}$; Bax^{KO} animals. Adult (8 week) animals were treated for 5 days and brains collected after 15 days (20-day post-tamoxifen treatment). White arrows indicate neurons that have lost BRN3A and express AP. Note that $Bm3a^{FloxAP}$ lacks AP staining since the Bm3a locus is not recombined in this condition. The box indicates the magnified area in the merged column and additionally the inset that shows an inverted, black/white image of the AP staining. A cluster of BRN3A(-)/AP(+) cells in the $Bm3a^{cKO}$; Bax^{KO} condition is delineated with an orange dashed line.

(G) Quantification of BRN3A expressing neurons and cell death (MH area and total number of DAPI nuclei). Different time points were analyzed: 0.5 and 2 days of tamoxifen treatment and 20 days post-tamoxifen treatment (5 days of treatment plus 15 days of wait). The histograms represent the MH area (blue dashed line area in BRN3A panels), the total number of DAPI within the MH area, and the percentage of BRN3A-epxressing neurons relative to the total number of DAPI nuclei for each respective genotype. Treated Bm3a^{FloxAP}, Bm3a^{cKO}, Bm3a^{cKO};BAX^{KO}, and Bm3a^{FloxWt};R26^{Cre};BAX^{KO} (as a control for the Bm3a^{cKO};BAX^{KO} condition) are shown (see also Figure S3). Significance was calculated using a one-way ANOVA, followed by a post-hoc Tukey's multiple comparisons test. * p <0.05; *** p <0.01; *** p <0.001. Only the significant differences with p <0.01 are annotated in the graph. See Table S2 for a summary of Brn3a expression in adult CNS and a summary of cell death phenotypes in distinct parts of the CNS. See Table S3 for details on the statistical comparisons of the quantified data. Scale bars represent 100 μm. Data represented as mean + SD.



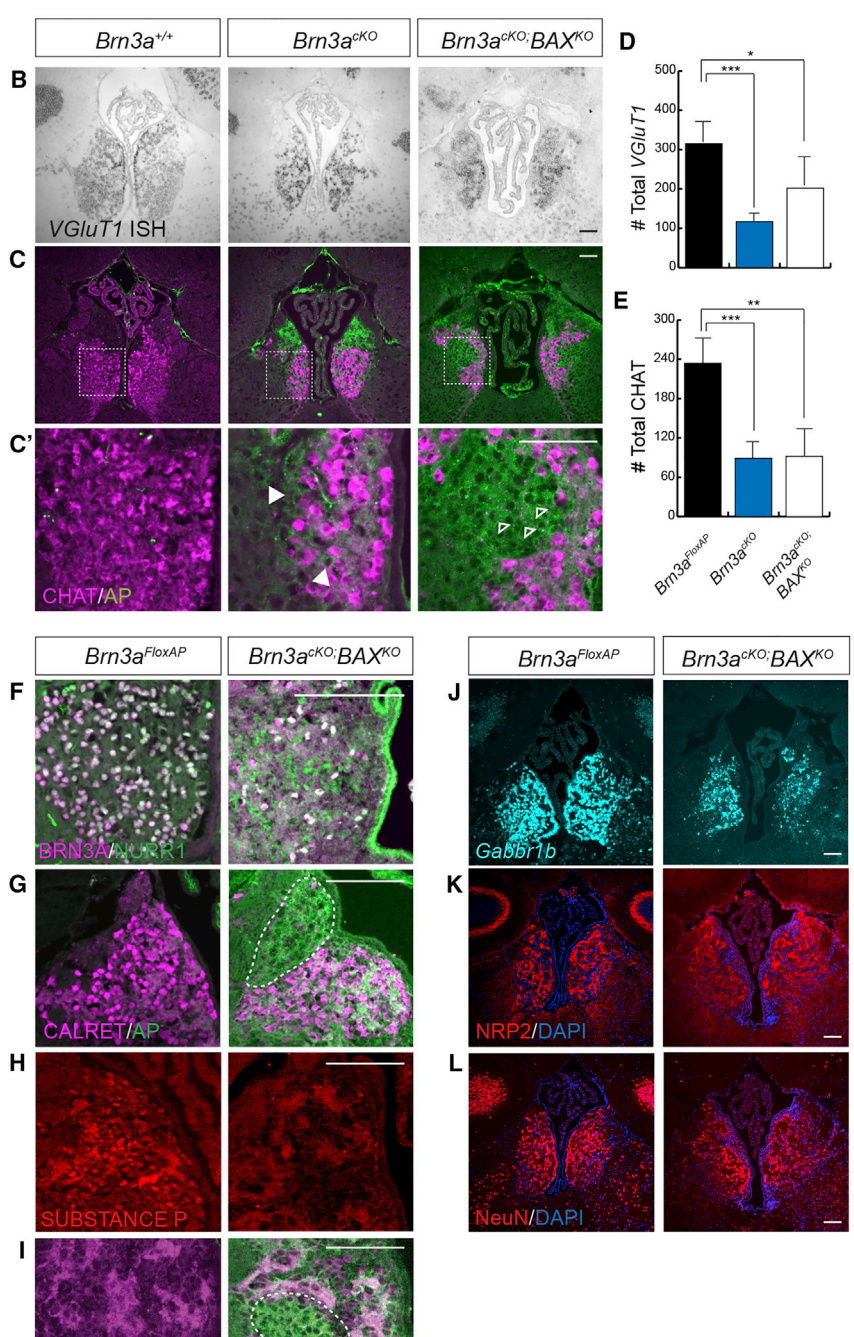


Figure 3. BRN3A Is Necessary for Maintaining the Expression of MH-Specific Terminal Markers, but Not Pan-neuronal Identity

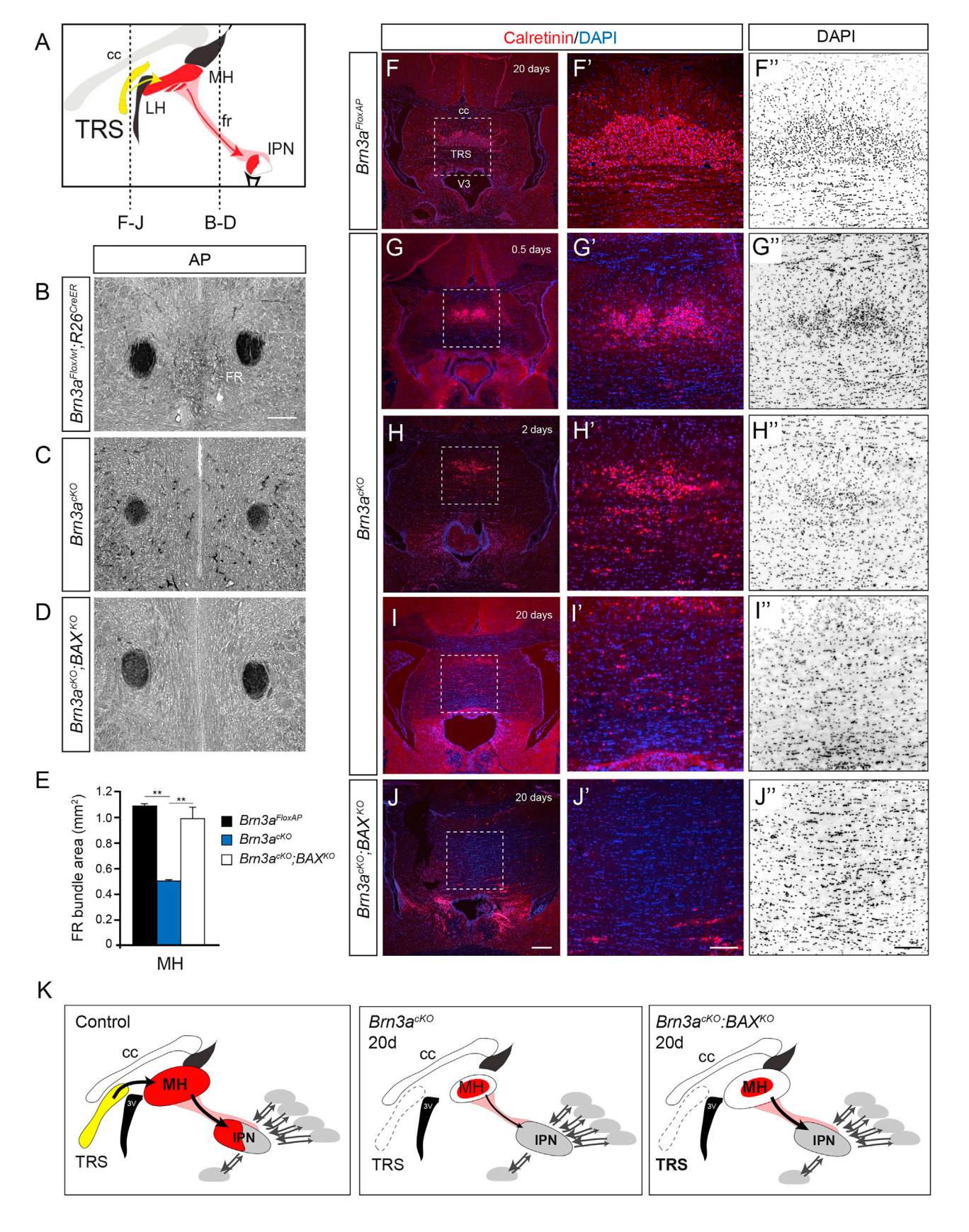
(A) Tabular summary of the markers analyzed in this study. The technique used to detect each marker is indicated (See STAR Methods for details). Some of these genes have been analyzed in a $\mathit{Brn3a}^{\mathit{KO}}$ background in a previous study [15] (n.d., not

(B-E) Neurotransmitter identity is affected after the adult removal of Brn3a in adult (8 weeks) animals. Neurotransmitter markers were tested in Brn3a^{FloxAP}, Brn3a^{cKO}, and Brn3a^{cKO};Bax^{KO} animals at 20 days post-tamoxifen treatment (5 days of tamoxifen treatment and 15 days of wait). (B) Glutamatergic identity is analyzed by VGluT1 in situ hybridization. (D) Quantification of the total VGluT1 positive cells in 20 days post-tamoxifen treated Brn3a^{FloxAP}, Brn3a^{cKO} and Brn3a^{cKO};Bax^{KO} animals. Significance was calculated with Student's t test. * p < 0.05; ** p <0.01. (C) Cholinergic identity is analyzed by co-labeling of CHAT and AP by antibody staining. (C') Magnification of the dashed inset in (C). In Bm3acKO, a few surviving neurons that express AP have lost CHAT expression (solid white arrow heads). In Brn3acKO; BaxKO, a cluster of AP(+) cells show no expression of CHAT. We have shown in Figure 2F that AP(+) cells have lost BRN3A expression. (E) Quantification of the total number of CHAT positive neurons within the MH. Significance was calculated with Student's t-test. * p < 0.05; ** p <0.01.

(F-J) Terminal markers expression is reduced after the adult removal of Brn3a. The different terminal markers were analyzed by antibody staining in Brn3a^{FloxAP} and Brn3a^{cKO};Bax^{KO} animals after 5 days of treatment and 15 days of wait (20 days post-tamoxifen treatment). (F) The expression of NURR1 is reduced after the adult removal of Brn3a. Co-labeling of NURR1 and BRN3A by antibody staining in 20 day post-treated (5 days of tamoxifen treatment and 15 days of wait) in $\mathit{Brn3a}^{\mathit{FloxAP}}$ and Brn3acKO;BaxKO. An inset of the ventral MH is shown. (G) Calretinin staining is affected in the dorsal MH. Only the dorsal MH is shown. The dashed line area in depicts a cluster of AP(+) cells where Calretinin is not detected. (H) Substance P staining is lost after the adult removal of Brn3a. The dorsal MH is shown. (I) KTCD8 staining is reduced in the ventral MH. A region of the ventral MH is shown. The dashed line area in indicates a cluster of AP(+) cells where KTCD8 is not detected. (J) Gabbr1b expression is reduced in the MH. Gabbr1b mRNA was detected using RNAscope® technology.

(K) NRP2 staining is not affected by the loss of BRN3A. NRP2 expression, analyzed by antibody staining in tamoxifen treated Brn3aFloxAP and $\mathit{Brn3a}^{\mathit{cKO}}$; $\mathit{Bax}^{\mathit{KO}}$ is not lost in the absence of BRN3A. (L) The pan-neuronal marker, NeuN is not affected by loss of BRN3A. NeuN antibody staining in tamoxifen treated Brn3a^{FloxAP} and Brn3a^{cKO};Bax^{KO}.

In (D) and (E), data represented as mean + SD. All markers were tested after 20 days post-tamoxifen treatment (5 days of treatment and 15 days of wait). At least n = 3 animals per condition were analyzed. Scale bars represent 100 µm.



habenulas, we found that 50% of neurons that normally express choline acetyltransferase (CHAT) fail to do so in *Brn3a^{cKO};Bax^{KO}* animals (Figures 3C and 3E). Apart from neurotransmitter identity, we tested whether *Brn3a* is required to maintain additional identity features of adult MH neurons. We analyzed markers that have been previously shown to require *Brn3a* for initiation of expression in the embryo [15] and markers that have been shown to be enriched in the MH according to the Allen Brain Atlas [34] (Figure 3A). By co-staining for terminal markers and for AP (which reflects recombination of the locus), we found that the expression of all these terminal identity markers is lost in *Brn3a^{cKO};Bax^{KO}* MH neurons 20 days after tamoxifen treatment, indicating that BRN3A is necessary for maintaining multiple terminal identity features in the adult MH neurons (Figures 3F–3J).

Previous studies in C. elegans reported that while terminal selector-type transcription factors (TFs), including unc-86, are responsible for the specification of neuron-class-specific terminal identity features [13], they do not regulate the general panneuronal characteristics of a neuron [11, 13, 35]. Similarly, we found that the loss of Brn3a in adult mouse brain did not affect the expression of the pan-neuronal marker NeuN in Brn3acKO; BaxKO animals (Figures 2C-2E and 3L). C. elegans terminal selectors, like unc-86, also do not affect the expression of broadly expressed axon guidance receptors [11, 13, 35]. Likewise, we found that the expression of the cell surface receptor Neuropilin 2 (NRP2) was not affected in Brn3a^{cKO};Bax^{KO} animals (Figure 3K) [15]. These findings generally parallel conclusions made from studies of various terminal selectors in C. elegans-namely, that terminal selectors selectively control neuron-type-specific, terminal identity features [35].

Loss of *Brn3a* in Adult Medial Habenular Neurons Does Not Affect MH Efferents

The MH neurons project to their target neurons in the interpeduncular nucleus (IPN) almost exclusively via the fasciculus retroflexus (FR) [27, 36] (Figure 4A). In *Bm3* null mutant, E12.5 embryos, the MH neurons reach the IPN, but shortly after, there is a profound defect in innervation, denoted by a reduced cross-sectional area of the FR [15]. We followed the same approach and measured the cross-sectional area of the FR fibers, marked by AP staining, in 20-day post-tamoxifen treatment adult control *Brn3a*^{FloxAP/wt};*R26*^{CreER} and in *Brn3a*^{CKO} and *Brn3a*^{CKO};*Bax*^{KO} animals (Figures 4B–4E and S3B). We found that the FR area is significantly reduced in *Brn3a*^{CKO}, which correlates with the increased cell death in the MH in these animals. However,

upon suppression of cell death in $Bm3a^{cKO}$; Bax^{KO} animals, the FR area is not significantly different from the control $Bm3a^{FloxAP/wt}$; $R26^{CreER}$ animals (Figure 2G, S3B, and S3C). This suggests that the loss of Bm3a in adult mice does not affect the maintenance of the MH-IPN projection.

Afferents to the MH Degenerate after Removal of Brn3a

The MH receives its afferent inputs mainly from the triangular nucleus of the septum (TRS) through the Stria Medularis [27, 37] (Figure 4A). The neurons of the TRS, which do not express Brn3a at any time point, are marked by Calretinin staining [34, 38]; their somata are located in the corpus callosum, forming a triangular cluster that is discernible by DAPI staining (Figure 4F). We found that $\mathit{Brn3a}^{\mathit{cKO}}$ animals, which display a severe loss of neurons in the MH (Figures 2D and S3D), show a progressive loss of Calretinin-positive neurons in the TRS area and eventually a complete loss of Calretinin-positive neurons at 20 days after tamoxifen treatment (Figures 4G-4I). In contrast, Calretininpositive cells in the corpus callosum were not affected by loss of Brn3a. The lack of Calretinin staining is likely due to the degeneration of the TRS neurons because we also did not observe the characteristic triangular cluster of cells by DAPI staining (Figure 4I).

Intriguingly, *Bm3a^{cKO};Bax^{KO}* animals, in which MH neurons remain alive but have lost their neurotransmitter identity, show a similar loss of Calretinin staining of TRS fibers and loss of DAPI signals (Figure 4J). These observations indicate that it is not only the physical removal of MH neurons by cell death, but also the loss of MH neuron identity that non-cell-autonomously affects innervating neurons. These results also indicate that the degeneration of the TRS nucleus in the absence of functional MH neurons is not controlled by the *Bax*-dependent mitochondrial cell death pathway. Taken together, we have shown that in a fully developed adult mouse brain, the loss of neuronal identity triggered by removal of an identity-maintaining transcription factor can lead to profound, non-cell-autonomous defects on neuronal circuit integrity in the adult brain.

Conclusions

Two orthologous POU homeobox genes, *C. elegans unc-86* and mouse *Brn3a*, both act as terminal selectors of neuronal identity. Previous work has shown that *unc-86* and *Brn3a* are required during development to initiate the terminal differentiation program of a number of different neuronal classes [7–13, 15–18]. In both worms and mice, the terminal gene batteries controlled by these POU homeobox genes are similar and include

Figure 4. Loss of Brn3a in the Adult Brain Affects the MH Connectivity

(A) Schematic of the triangular septum (TRS)-medial habenula (MH)-interpeduncular nucleus (IPN) circuit.

(B–D) The innervation to the IPN is reduced as a consequence of MH neurodegeneration. Coronal cross-section of the Fasciculus Retroflexus (FR) bundle at the level of the thalamus (B-D in the schematic) in Bm3a^{FloxAP/wt};R26^{CreER}, Bm3a^{CKO}, and Bm3a^{CKO};Bax^{KO} adult (8 week) animals treated for 20 days (5 days of tamoxifen treatment and 15 days of wait). See also Figure S3.

(E) Quantification of the FR cross-section area. n = 3 brains per genotype. Significance was calculated using a one-way ANOVA test with Tukey's post hoc analysis, ** p <0.01. Data represented as mean + SEM. See also Figure S3.

(F–J) Non-cell-autonomous degeneration of the TRS as a consequence of the MH neurodegeneration and the MH loss of identity. Different time points were analyzed: 0.5 and 2 days of tamoxifen treatment and 5 days of treatment plus 15 days of wait. Calretinin antibody staining is shown in the left and middle rows (F–J'). The inset is magnified in the middle and right rows (F'–J''). DAPI staining in Bm3a^{FloxAP}, Bm3a^{cKO}; Bax^{KO} animals at the level of the TRS (F"–J" in the schematic).

(K) Model illustrating the phenotypes observed in the TRS-MH-IPN circuit after the neurodegeneration of MH neurons (indicated by smaller size of circled MH area) or the loss of MH identity (indicated by red filling which is decreased in mutant conditions). Scale bars represent 1 mm (B–D) and 500 μm (F–J).

neurotransmitter identity, neuropeptide expression, and ion channel-encoding genes, i.e., genes whose products define the functional state of a differentiated neuron. We have shown here that these transcription factors also serve to maintain the differentiated state of neurons and therefore represent the regulatory endpoint of neuronal identity control. Both *unc-86* and *Brn3a*, as well as many other transcription factors classified as terminal selectors, are dedicated to controlling neuron-type-specific features, whereas generic, pan-neuronal features are not controlled by *unc-86*, *Bm3a*, or other terminal selectors [35]. Thus, the acquisition of pan-neuronal identity and the acquisition of neuron-type-specific features are genetically separable.

The MH is comprised of a number of different neuronal subtypes that are present in different areas of the MH [33]. Brn3a affects both the initial specification and maintenance of all different subtypes and we assume that the specificity of Brn3a function is determined by its subtype-specific interaction with distinct TFs. Several TFs are indeed expressed in the adult MH [34, 39], and at least one of them, NURR1, has been shown to functionally cooperate with BRN3A in the specification of MH neuronal subtypes [15]. The activity of subtype-specific cofactors could also explain the incomplete penetrance of the Brn3a mutant phenotype that we described here. Subtypespecific partnering of mouse Brn3a with other transcription factors is also very reminiscent of C. elegans unc-86, which specifies the identity of related neurons through the interaction with neuron-class-specific cofactors [8, 10-13, 40]. In some of these cases, removal of unc-86 alone shows partially penetrant phenotype, and it is only the joint removal of unc-86 and its cofactor that results in fully penetrant loss-of-identity phenotypes [8, 11]. The existence of neuron-type-specific cofactors is also the likely explanation for why BRN3A function differs in distinct parts of the CNS. For example, in contrast to the medial habenula, removal of BRN3A in the adult animal does not affect the survival of retinal ganglion cells, but the LIM homeobox ISL1, co-expressed with BRN3A in these cells, but not the medial habenula, may compensate for the loss of BRN3A in the retinal ganglion cells [41].

Adult neurons are generally more resistant to a number of cues that promote cell death during development [42]. How this increased resistance is regulated is not well understood. We have shown here that one of the consequences of removing Brn3a in adult animals is the loss of MH neurons via BAX-dependent cell death, indicating that adult neurons do retain the ability to undergo apoptosis under specific circumstances. Apoptosis parallels the loss of cellular identity upon Brn3a removal, but it is presently not clear whether the observed apoptosis is a secondary consequence of loss of neuronal identity features or whether cell survival is controlled by Brn3a in parallel to its control of terminal identity features of mature neurons. In either case, the link of neuronal identity and cell survival may constitute a "check point" mechanism by which it is ensured that a cell will only survive if its terminal differentiation program is properly executed and maintained.

We have also shown that the septal neurons providing afferents to the MH neurons die as a consequence of MH neurodegeneration or the loss of MH identity. These results suggest that, in adult animals, the septal neurons depend not only on the presence of their target neurons, but also on the specific

identity of their targets. Even though it is well known that target cells regulate the survival of afferent neurons during development [43], a similar dependency has, to our knowledge, not yet been described in the adult CNS. To the contrary, as mentioned above, neurons are generally thought to readjust their control of cell death pathways once they progress to the adult stage [42]. For example, in early developmental stages, the survival of inferior olivary neurons depend on their Purkinje neuron target cells, but this dependency disappears in later life [44]. In the case of the septal-medial habenular pathway, the susceptibility to target-derived trophic support may be retained through adult stages. In line with the unusual and novel target dependency of septal neuron survival, we find that the cell death of the septal afferents observed upon MH identity loss is not prevented by inhibiting BAX-dependent apoptosis (i.e. the death is still observed in Brn3acKO;BaxKO animals) and may be regulated by non-apoptotic pathways. Taken together, our findings indicate that in vertebrates, the maintenance of neuronal identity does not only entail continuous transcriptional activation of "neuron function genes" (transmitters, channels, etc.), but also the active prevention of the cell death. The coupling of neuronal identity maintenance with neuron survival in the adult nervous system is apparently absent in the C. elegans (i.e., neurons that fail to acquire or maintain their identity do not undergo cell death [35]), which correlates with the notion that neuron survival in C. elegans also does not depend on trophic signals during development and neuronal circuit formation [45].

STAR*METHODS

Detailed methods are provided in the online version of this paper and include the following:

- KEY RESOURCE TABLE
- CONTACT FOR REAGENT AND RESOURCE SHARING
- EXPERIMENTAL MODEL AND SUBJECT DETAILS
- METHOD DETAILS
 - C. elegans microscopy
 - O Targeted genome modification in *C. elegans*
 - Temporally controlled protein degradation in C. elegans
 - O Temporally controlled gene deletion in mice
 - Mouse histology and staining
- QUANTIFICATION AND STATISTICAL ANALYSIS

SUPPLEMENTAL INFORMATION

Supplemental Information includes three figures and three tables and can be found with this article online at https://doi.org/10.1016/j.cub.2018.06.045.

ACKNOWLEDGEMENTS

We thank Qi Chen for generating transgenic strains; Quifa Ma for RNA probes; Tudor Badea for providing mouse strains, advice, and discussion; Bernhard Bettler and Carol Mason for providing antibodies; and Rafael Yuste, Evan Deneris, Tudor Badea, Hynek Witchterle, and members of the Hobert lab for comments on the manuscript. E.S.-S. was funded by a Young Investigator Award from the Brain and Behavior Research Foundation and E.L.-D. was funded by a postdoctoral fellowship from the EMBO. O.H. is an Investigator of the Howard Hughes Medical Institute. This work was supported by NIH U01 MH105924.

AUTHOR CONTRIBUTIONS

E.S.-S. and O.H. conceived the project. E.L.-D. generated the conditional *unc-86* allele and performed the experiments for the *C. elegans* section and the Fasciculus Retroflexus AP staining and quantification. E.S.-S. performed the medial habenula and septum imaging and quantifications. E.D.L.C. provided technical support. E.D.L.C., E.S.-S., and E.L.-D. performed the mouse tamoxifen treatments, perfusion, and colony maintenance (breeding and genotyping). The manuscript was prepared by E.S.-S., E.L.-D. and O.H.

DECLARATIONS OF INTEREST

The authors declare no conflict of interest.

Received: May 13, 2018 Revised: June 8, 2018 Accepted: June 19, 2018 Published: August 23, 2018

REFERENCES

- Blau, H.M. (1992). Differentiation requires continuous active control. Annu. Rev. Biochem. 61, 1213–1230.
- Holmberg, J., and Perlmann, T. (2012). Maintaining differentiated cellular identity. Nat. Rev. Genet. 13, 429–439.
- Deneris, E.S., and Hobert, O. (2014). Maintenance of postmitotic neuronal cell identity. Nat. Neurosci. 17, 899–907.
- Finney, M., Ruvkun, G., and Horvitz, H.R. (1988). The C. elegans cell lineage and differentiation gene unc-86 encodes a protein with a homeodomain and extended similarity to transcription factors. Cell 55, 757–769.
- Finney, M., and Ruvkun, G. (1990). The unc-86 gene product couples cell lineage and cell identity in C. elegans. Cell 63, 895–905.
- Chalfie, M., Horvitz, H.R., and Sulston, J.E. (1981). Mutations that lead to reiterations in the cell lineages of C. elegans. Cell 24, 59–69.
- Sze, J.Y., Zhang, S., Li, J., and Ruvkun, G. (2002). The C. elegans POUdomain transcription factor UNC-86 regulates the tph-1 tryptophan hydroxylase gene and neurite outgrowth in specific serotonergic neurons. Development 129, 3901–3911.
- Serrano-Saiz, E., Poole, R.J., Felton, T., Zhang, F., De La Cruz, E.D., and Hobert, O. (2013). Modular control of glutamatergic neuronal identity in C. elegans by distinct homeodomain proteins. Cell 155, 659–673.
- Pereira, L., Kratsios, P., Serrano-Saiz, E., Sheftel, H., Mayo, A.E., Hall, D.H., White, J.G., LeBoeuf, B., Garcia, L.R., Alon, U., and Hobert, O. (2015). A cellular and regulatory map of the cholinergic nervous system of C. elegans. eLife 4, e12432.
- Lloret-Fernández, C., Maicas, M., Mora-Martínez, C., Artacho, A., Jimeno-Martín, Á., Chirivella, L., Weinberg, P., and Flames, N. (2018). A transcription factor collective defines the HSN serotonergic neuron regulatory landscape. eLife 7, e32785.
- 11. Zhang, F., Bhattacharya, A., Nelson, J.C., Abe, N., Gordon, P., Lloret-Fernandez, C., Maicas, M., Flames, N., Mann, R.S., Colón-Ramos, D.A., and Hobert, O. (2014). The LIM and POU homeobox genes ttx-3 and unc-86 act as terminal selectors in distinct cholinergic and serotonergic neuron types. Development 141, 422–435.
- Duggan, A., Ma, C., and Chalfie, M. (1998). Regulation of touch receptor differentiation by the Caenorhabditis elegans mec-3 and unc-86 genes. Development 125, 4107–4119.
- Gordon, P.M., and Hobert, O. (2015). A competition mechanism for a homeotic neuron identity transformation in C. elegans. Dev. Cell 34, 206–219.
- Xiang, M., Gan, L., Zhou, L., Klein, W.H., and Nathans, J. (1996). Targeted deletion of the mouse POU domain gene Brn-3a causes selective loss of neurons in the brainstem and trigeminal ganglion, uncoordinated limb movement, and impaired suckling. Proc. Natl. Acad. Sci. USA 93, 11950–11955.

- Quina, L.A., Wang, S., Ng, L., and Turner, E.E. (2009). Brn3a and Nurr1 mediate a gene regulatory pathway for habenula development. J. Neurosci. 29, 14309–14322.
- Badea, T.C., Cahill, H., Ecker, J., Hattar, S., and Nathans, J. (2009).
 Distinct roles of transcription factors brn3a and brn3b in controlling the development, morphology, and function of retinal ganglion cells. Neuron 61, 852–864.
- Dykes, I.M., Tempest, L., Lee, S.I., and Turner, E.E. (2011). Brn3a and Islet1 act epistatically to regulate the gene expression program of sensory differentiation. J. Neurosci. 31, 9789–9799.
- Dykes, I.M., Lanier, J., Eng, S.R., and Turner, E.E. (2010). Brn3a regulates neuronal subtype specification in the trigeminal ganglion by promoting Runx expression during sensory differentiation. Neural Dev. 5, 3.
- Eng, S.R., Dykes, I.M., Lanier, J., Fedtsova, N., and Turner, E.E. (2007).
 POU-domain factor Brn3a regulates both distinct and common programs of gene expression in the spinal and trigeminal sensory ganglia. Neural Dev. 2. 3.
- Hsu, Y.W., Wang, S.D., Wang, S., Morton, G., Zariwala, H.A., de la Iglesia, H.O., and Turner, E.E. (2014). Role of the dorsal medial habenula in the regulation of voluntary activity, motor function, hedonic state, and primary reinforcement. J. Neurosci. 34, 11366–11384.
- Notredame, C., Higgins, D.G., and Heringa, J. (2000). T-Coffee: A novel method for fast and accurate multiple sequence alignment. J. Mol. Biol. 302, 205–217.
- Gold, D.A., Gates, R.D., and Jacobs, D.K. (2014). The early expansion and evolutionary dynamics of POU class genes. Mol. Biol. Evol. 31, 3136– 3147
- Baumeister, R., Liu, Y., and Ruvkun, G. (1996). Lineage-specific regulators couple cell lineage asymmetry to the transcription of the Caenorhabditis elegans POU gene unc-86 during neurogenesis. Genes Dev. 10, 1395– 1410
- Zhang, L., Ward, J.D., Cheng, Z., and Dernburg, A.F. (2015). The auxin-inducible degradation (AID) system enables versatile conditional protein depletion in C. elegans. Development 142, 4374–4384.
- Dickinson, D.J., Pani, A.M., Heppert, J.K., Higgins, C.D., and Goldstein, B. (2015). Streamlined Genome Engineering with a Self-Excising Drug Selection Cassette. Genetics 200, 1035–1049.
- Xiang, M., Zhou, L., Macke, J.P., Yoshioka, T., Hendry, S.H., Eddy, R.L., Shows, T.B., and Nathans, J. (1995). The Brn-3 family of POU-domain factors: primary structure, binding specificity, and expression in subsets of retinal ganglion cells and somatosensory neurons. J. Neurosci. 15, 4762–4785.
- Schmidt, E.R.E., and Pasterkamp, R.J. (2017). The molecular mechanisms controlling morphogenesis and wiring of the habenula. Pharmacol. Biochem. Behav. 162, 29–37.
- Gampe, K., Hammer, K., Kittel, Á., and Zimmermann, H. (2012). The medial habenula contains a specific nonstellate subtype of astrocyte expressing the ectonucleotidase NTPDase2. Glia 60, 1860–1870.
- Badea, T.C., Wang, Y., and Nathans, J. (2003). A noninvasive genetic/ pharmacologic strategy for visualizing cell morphology and clonal relationships in the mouse. J. Neurosci. 23, 2314–2322.
- Knudson, C.M., Tung, K.S., Tourtellotte, W.G., Brown, G.A., and Korsmeyer, S.J. (1995). Bax-deficient mice with lymphoid hyperplasia and male germ cell death. Science 270, 96–99.
- Renault, T.T., and Manon, S. (2011). Bax: Addressed to kill. Biochimie 93, 1379–1391.
- Ren, J., Qin, C., Hu, F., Tan, J., Qiu, L., Zhao, S., Feng, G., and Luo, M. (2011). Habenula "cholinergic" neurons co-release glutamate and acetylcholine and activate postsynaptic neurons via distinct transmission modes. Neuron 69, 445–452.
- Aizawa, H., Kobayashi, M., Tanaka, S., Fukai, T., and Okamoto, H. (2012).
 Molecular characterization of the subnuclei in rat habenula. J. Comp. Neurol. 520, 4051–4066.

- 34. Lein, E.S., Hawrylycz, M.J., Ao, N., Ayres, M., Bensinger, A., Bernard, A., Boe, A.F., Boguski, M.S., Brockway, K.S., Byrnes, E.J., et al. (2007). Genome-wide atlas of gene expression in the adult mouse brain. Nature 445, 168–176.
- Hobert, O. (2016). Terminal Selectors of Neuronal Identity. Curr. Top. Dev. Biol. 116, 455–475.
- Molas, S., DeGroot, S.R., Zhao-Shea, R., and Tapper, A.R. (2017).
 Anxiety and Nicotine Dependence: Emerging Role of the Habenulo-Interpeduncular Axis. Trends Pharmacol. Sci. 38, 169–180.
- Swanson, L.W., and Cowan, W.M. (1979). The connections of the septal region in the rat. J. Comp. Neurol. 186, 621–655.
- Rogers, J.H., and Résibois, A. (1992). Calretinin and calbindin-D28k in rat brain: patterns of partial co-localization. Neuroscience 51, 843–865.
- Görlich, A., Antolin-Fontes, B., Ables, J.L., Frahm, S., Slimak, M.A., Dougherty, J.D., and Ibañez-Tallon, I. (2013). Reexposure to nicotine during withdrawal increases the pacemaking activity of cholinergic habenular neurons. Proc. Natl. Acad. Sci. USA 110, 17077–17082.
- Xue, D., Finney, M., Ruvkun, G., and Chalfie, M. (1992). Regulation of the mec-3 gene by the C.elegans homeoproteins UNC-86 and MEC-3. EMBO J. 11, 4969–4979.
- Huang, L., Hu, F., Xie, X., Harder, J., Fernandes, K., Zeng, X.Y., Libby, R., and Gan, L. (2014). Pou4f1 and pou4f2 are dispensable for the long-term survival of adult retinal ganglion cells in mice. PLoS ONE 9, e94173.
- 42. Kole, A.J., Annis, R.P., and Deshmukh, M. (2013). Mature neurons: equipped for survival. Cell Death Dis. 4, e689.
- Sofroniew, M.V., Galletly, N.P., Isacson, O., and Svendsen, C.N. (1990). Survival of adult basal forebrain cholinergic neurons after loss of target neurons. Science 247, 338–342.
- Zanjani, H., Lemaigre-Dubreuil, Y., Tillakaratne, N.J., Blokhin, A., McMahon, R.P., Tobin, A.J., Vogel, M.W., and Mariani, J. (2004). Cerebellar Purkinje cell loss in aging Hu-Bcl-2 transgenic mice. J. Comp. Neurol. 475, 481–492.

- Jaaro, H., Beck, G., Conticello, S.G., and Fainzilber, M. (2001). Evolving better brains: a need for neurotrophins? Trends Neurosci. 24, 79–85.
- Serrano-Saiz, E., Pereira, L., Gendrel, M., Aghayeva, U., Battacharya, A., Howell, K., Garcia, L.R., and Hobert, O. (2017). A Neurotransmitter Atlas of the *Caenorhabditis elegans* Male Nervous System Reveals Sexually Dimorphic Neurotransmitter Usage. Genetics 206, 1251–1269.
- Serrano-Saiz, E., Oren-Suissa, M., Bayer, E.A., and Hobert, O. (2017).
 Sexually Dimorphic Differentiation of a C. elegans Hub Neuron Is Cell Autonomously Controlled by a Conserved Transcription Factor. Curr. Biol. 27, 199–209.
- Brenner, S. (1974). The genetics of Caenorhabditis elegans. Genetics 77, 71–94.
- Schneider, C.A., Rasband, W.S., and Eliceiri, K.W. (2012). NIH Image to ImageJ: 25 years of image analysis. Nat. Methods 9, 671–675.
- Kerk, S.Y., Kratsios, P., Hart, M., Mourao, R., and Hobert, O. (2017).
 Diversification of C. elegans Motor Neuron Identity via Selective Effector Gene Repression. Neuron 93. 80–98.
- Fedtsova, N.G., and Turner, E.E. (1995). Brn-3.0 expression identifies early post-mitotic CNS neurons and sensory neural precursors. Mech. Dev. 53, 291–304.
- Flames, N., Pla, R., Gelman, D.M., Rubenstein, J.L., Puelles, L., and Marín, O. (2007). Delineation of multiple subpallial progenitor domains by the combinatorial expression of transcriptional codes. J. Neurosci. 27, 9682–9695.
- 53. Cheng, L., Arata, A., Mizuguchi, R., Qian, Y., Karunaratne, A., Gray, P.A., Arata, S., Shirasawa, S., Bouchard, M., Luo, P., et al. (2004). Tlx3 and Tlx1 are post-mitotic selector genes determining glutamatergic over GABAergic cell fates. Nat. Neurosci. 7, 510–517.
- Schindelin, J., Arganda-Carreras, I., Frise, E., Kaynig, V., Longair, M., Pietzsch, T., Preibisch, S., Rueden, C., Saalfeld, S., Schmid, B., et al. (2012). Fiji: an open-source platform for biological-image analysis. Nat. Methods 9, 676–682.

STAR*METHODS

KEY RESOURCE TABLE

DEACENT ANDECOLIDEE	COLIDOE	IDENTIFIED
REAGENT or RESOURCE	SOURCE	IDENTIFIER
Antibodies		
anti-BRN3A (Mouse) (1/50 concentration)	Santa Cruz	Cat#sc-8429; RRID: AB_626765
anti-BRN3A (Rabbit) (1/2000 concentration)	Gift form C. Mason	N/A
anti-CHAT (Goat) (1/100 concentration)	Millipore	Cat#AB144; RRID: AB_90650
anti-NeuN (Rabbit) (1/500 concentration)	Millipore	Cat#ABN78; RRID: AB_10807945
anti-Alkaline Phosphatase (Mouse) (1/100 concentration)	BioRad	Cat#MCA2091; RRID: AB_2226283
anti-Calretinin (Rabbit) (1/2000 concentration)	Swant	Cat#7697; RRID: AB_261910
anti-Neuropilin 2 (Goat) (1/200 concentration)	R&D	Cat#AF567; RRID: AB_215523
anti-Substance P (Rat) (1/100 concentration)	Millipore	Cat#MAB356; RRID: AB_94639
anti-KTCD8 (Rabbit) (1/500 concentration)	Gift from B. Bettler	N/A
anti-NURR1 (Goat) (1/100 concentration)	R&D Systems	Cat#AF2156; RRID: AB_2153894
anti-Alexa-488 anti-Mouse (Donkey) (1/500 concentration)	ThermoFisher	Cat#A-21202; RRID: AB_141607
anti-Alexa-594 anti-Mouse (Donkey) (1/500 concentration)	ThermoFisher	Cat#A-21203: RRID: AB_2535789
anti-Alexa-488 anti-Rabbit (Goat) (1/500 concentration)	ThermoFisher	Cat#A-11008; RRID: AB_143165
anti-Cy™3 anti-Rabbit (Donkey) (1/500 concentration)	Jackson ImmunoResearch	Cat#711-165-152; RRID: AB_2307443
anti-Cy™5 anti-Goat (Donkey) (1/500 concentration)	Jackson ImmunoResearch	Cat#705-175-147; RRID: AB_2340415
anti-Cy™3 anti-Rat (Donkey) (1/500 concentration)	Jackson ImmunoResearch	Cat#712-165-150: RRID: AB_2340666

CONTACT FOR REAGENT AND RESOURCE SHARING

Further information and requests for resources and reagents should be directed to and will be fulfilled by the Lead Contact, Oliver Hobert (or38@columbia.edu). Strains can be requested from the Caenorhabditis Genetics Center.

EXPERIMENTAL MODEL AND SUBJECT DETAILS

The C. elegans transgenic strains used in this study were OH15227 (unc-86(ot893)[unc-86::mNG::AID])(generated in this study), CA1200 (ieSi57[eft-3^{prom}::TIR1]) [24], OH13646 (otIs544[cho-1^{fosmid}::sl2::mChOpti::h2b]) [9], OH12495 (otIs517[tph-1^{fosmid}:: sl2::yfp::h2b]) [46], OH13645 (otls518[eat-4^{fosmid}::sl2::mChOpti::h2b]) [47] and OH4841(otls92[flp-10^{prom}::gfp]). Animals were maintained at 20C with abundant E. coli OP50 as food following standard conditions [48].

The mouse strains used in this study were Cre line Rosa26^{CreER} [16], the conditional Brn3a^{FloxAP} allele [16] and the targeted deletion Bax^{KO} allele [30]. The conditional Brn3a^{cKO} was generated by crossing Rosa26^{CreER} and Brn3a^{FloxAP}. The line Brn3a^{cKO};Bax^{KO} is maintained by crossing males Brn3a^{cKO} with females Brn3a^{cKO};Bax^{KO/wt}. All experiments were performed on 8~10-week-old mice. Mice were raised in 12-hr light/dark cycle in standard laboratory cages and given ad libitum access to food and water. All procedures and animal care followed the regulation and guidelines of the Institutional Animal Care and Use Committees (IACUC) of Columbia University.

METHOD DETAILS

C. elegans microscopy

Worms were anesthetized using 100 mM sodium azide (NaN₃) and mounted on 5% agarose pads on glass slides. Images were acquired using a Zeiss confocal microscope (LSM880). Several Z-stack images (each \sim 0.7 μ m thick) were acquired with the ZEN software. Images were reconstructed via maximum intensity Z-projection of 2-10 μm Z-stacks using the ImageJ software [49]. Representative images are shown following orthogonal projection of 2–10 μm Z-stacks.

Targeted genome modification in C. elegans

We had previously generated an mNeonGreen::AID cassette (mNG::AID) to tag endogenous genes via CRISPR/Cas9-mediated genome engineering for temporally controlled degradation [50]. In this cassette, codon-optimized mNeonGreen [25] is directly fused to the 45 amino acid long Auxin-Inducible Degron (AID) [24]. This cassette was placed into the pDD268 vector, which contains a self-excising drug selection cassette used for CRISPR/Cas9 genome engineering [25]. The cassette was inserted right before the stop codon of the *unc-86* locus, using a guide RNA that targets a sequence overlapping the *unc-86* locus STOP codon (target sequence: GGATTCTTTGATTAGTTTCG).

Temporally controlled protein degradation in C. elegans

Conditional protein depletion using the auxin-inducible degradation system in *C. elegans* was first reported in [24]. The conditional mutant allele *unc-86(ot893)[unc-86::mNG::AID]* was crossed with *ieSi57[eft-3^{prom}::TIR1]* to generate the experimental strains. The natural auxin, indole-3-acetic acid (IAA), was dissolved in ethanol (EtOH) to prepare 400 mM stock solutions which were stored at 4°C for up to one month. NGM (Nematode Growth Medium) agar plates with fully grown OP50 bacterial lawn were coated with the auxin stock solution to a final concentration of 4 mM and allowed to dry overnight at room temperature. To induce protein degradation, worms of the experimental strains were transferred onto the auxin-coated plates and kept at 20°C. As a control, worms were transferred onto EtOH-coated plates instead. Auxin solutions, auxin-coated plates, and experimental plates were shielded from light.

Temporally controlled gene deletion in mice

Tamoxifen was administered in the diet (TD.130857; Envigo) at a concentration of 80mg/kg/day. Adult (8 week) animals were fed with tamoxifen diet for 0.5 days or 2 days, and immediately after the animals were perfused and brains collected. For the 20 day post-treatment condition, animals were fed for 5 consecutive days with tamoxifen diet (Figure 2B). Then, it was replaced with regular diet for 15 more days. At that time the animals were perfused and brains collected.

Mouse histology and staining

After treatment, animals were perfused with 4% paraformaldehyde (PFA). The brains were post-fixed overnight in 4% PFA, washed in PBS and lastly embedded in Tissue-Tek O.C.T. Compound (VWR) for immunohistochemistry, alkaline phosphatase staining and *in situ* hybridization techniques. Brains were coronally sectioned at 16 μm thickness with a cryostat.

For immunofluorescence, sections were washed from OCT for 20 min in PBS-Triton X-100 at 0.05% (PBST). Sections were blocked for 45 min at room temperature with 1% BSA in PBS-Triton X-100 0.1%. Primary antibodies were diluted in PBS-Triton X-100 0.1% with 0.1% BSA (antibody solution). Incubations were done overnight at 4°C. The following day, samples were washed three times with PBST and incubated with the respective secondary antibodies (1/1000 in antibody solution) for 2 hr at room temperature. Sections were then washed 3 times in PBST, stained with DAPI for 5 min, washed with PBS and mounted with Clear-mount mounting media (17985-12, EMS). For a list of antibodies and concentrations see Key Resource Table. Images were taken using an automated fluorescence microscope (Zeiss, Axio Imager Z1 Stand). Image acquisition was performed with the Zen software from Zeiss microscopy.

To detect BRN3A we used two different antibodies: a commercial antibody obtained from Santa Cruz Biotech (sc-8429) and a polyclonal antibody previously characterized to be specific for BRN3A [51] (See Key Resource Table).

For standard *in situ* hybridization procedure, sections were hybridized with digoxigenin-conjugated probes as described previously [52]. The *VGluT1* probe was a gift from Quifu Ma. A fragment of 710 bp of *VGluT1* cDNA was cloned into pCRII vector [53]. We used the RNAscope® Florescence v2 Multiplex Assay (Cat No: 323110) *in situ* hybridization technique to detect three mRNA simultaneously. We used the pre-labeled probe *Gabbr1b* (Cat No: 425181-Channel 3).

For Alkaline Phosphatase staining, cryostat 16 μ m sections were incubated at 70°C for 1 hr in PBS-Tween-20 (0.1%) to inactivate endogenous phosphatases. Next, the sections were equilibrated in NTMT solution (100 mM Tris, pH 9.5, 100 mM NaCl, 50 mM MgCl₂, 0.1% Tween-20) for 10 min. Then sections were incubated in developing buffer (NTMT solution with 250 μ g/ml nitroblue tetrazolium, and 130 μ g/ml 5-bromo-4-chloro-3-indolyl phosphate) for 1 hr at room temperature. The reaction was stopped transferring the samples to PBS.

QUANTIFICATION AND STATISTICAL ANALYSIS

For the cell quantifications in mice, sections were selected at the same rostro-caudal level. The hippocampus was used as a reference. The Medial Habenula area has a distinct morphology that is retain even in $Brn3a^{cKO}$ mutant animals allowing us to define the MH area. Moreover, in the control animals (tamoxifen treated $Brn3a^{FloxAP}$), when we quantified the percentage of BRN3A neurons relative to total number of cells (DAPI nuclei) at different levels within the rostro-caudal axis, we observed always that 85% of cells were positive for BRN3A (data not shown).

The area of the Medial Habenula was quantified using Fiji [54] and plotted in μ m²/1000. The total number of DAPI nuclei, BRN3A and NeuN positive cells was acquired using the cell counter plug-in in Fiji. The data were analyzed with parametric tests, t test and one-way ANOVA followed by post-hoc Tukey's multiple comparisons test when data sets met assumptions of normality.